Experimental Study on Design Method of Real-sized Mobile Bridge for Moving Vehicle

Yuki Chikahiro[1], Ichiro Ario[1], Masatoshi Nakazawa[2], Syuichi Ono[3], Jan Holnicki-Szulc[4], Piotr Pawlowski[4] & Cezary Graczykowski[4]

[1]*Dept. of Civil & Environmental Engineering, Hiroshima University, Hiroshima, Japan*

[2] *Dept. of Civil & Environmental Engineering, Tohoku Gakuin University, Miyagi, Japan*

[3]*Japan Construction Method and Machinery Research Institute, Sizuoka, Japan*

[4]*Institute of Fundamental Technological Research, Dept. of Intelligent Technologies, Warsaw, Poland*

Abstract

Many natural disasters cause not only critical situations for facilities and resident's life, but also significant damage to economy. It is obvious that quick rescue action must be undertaken and that there are many problems due to the occurrence of secondary disasters at rescue worksite. Basing on the previous study of deployable structures and the concept of the multi-folding micro-structures, we propose a new type of foldable bridge in form of scissor structure called the Mobile Bridge^{TM}. In this paper, we discuss the vehicle passing test performed on the real-scale Mobile Bridge in order to evaluate its mechanical characteristics and application limits. Moreover, we verified the compatibility between the result of calculations and experiments by means of theoretical modelling. The results show that it is sufficient to treat the load as equivalent nodal forces applied at the joints without including the stiffness of the deck.

Keywords: Mobile Bridge^{TM}, Scissors type of emergency bridge, Aluminium alloy materials, Vehicle loading test

1 Introduction

In recent years, the world has seen many kinds of natural disasters such as earthquakes, floods and tsunamis. In a case of our floods investigation, many residents suffered from bridge and road damage caused by a very large flood along several branches of the Yamakuni River in northern Kyushu of Japan in 2012. Therefore, bridge designers or engineers have to consider how to rebuild the damaged infrastructure, and how to build new types of rescue systems, which can be quickly deployed, because rescue time is very important when trying to save lives in an emergency.

Based on the previous study of the previous study of deployable structures and *the concept* of the multi-folding micro-structures (1-4), we propose a new type of emergency bridge - the Mobile Bridge^{TM} (hereinafter-called MB) which can expand and store for concrete disaster recovery system (5). Although the upper and lower chord members are main elements which resist the bending moment in a general truss bridge, MB can be built by using a scissors mechanism for a bridge formation and resist to the sectional force in spite of lacking the one member (6-9).

Scissors structure which is the basis of the MB is typical for deployable structures which provide good storage and transportation performance. This structural form combines the members in the shape of X. The joint which connects the members of scissors is a pin-junction in form of a flexible hinge, and the pin joining sections called a "pivot" which exists in the central portion of a scissors member intersect.

This kind of scissors type bridge, provides several advantages: 1) even if there are few members for constructing, deployment and storage work are quickly, 2) assembling, transportation and disassembling is easy 3) it has high deployment performance because the scissors structure can deploy and store all units by one control force,.

In this paper, we discuss a vehicle loading test performed on the real-scaled Mobile Bridge (called MB1.0) in order to evaluate its mechanical characteristics and application limits. Moreover, we verify the compatibility between the result of analysis, and experiments by means of theoretical approach.

2 Outline of the real- scaled Mobile Bridge

The schematic view of the experimental, two-unit scissors model for a real scale mobile bridge (called as MB1.0) is shown in Fig.1. When deployment starts from the stored state, the members are sloped gradually until the full span is reached. Moreover, because the deck is sated in MB1.0, the deck works with member as deployment progresses.

In the final stage of expansion the scissors deployment angle is 60 degrees. The total length of the span is 7.0m and the height of the bridge is 2.0m. The total weight of the bridge including structural parts such as main members, shafts, and pins is 8.4kN. The aluminum alloy components are made of the three-chamber hollow section, which uses A6N01 material, is used for the main member, the

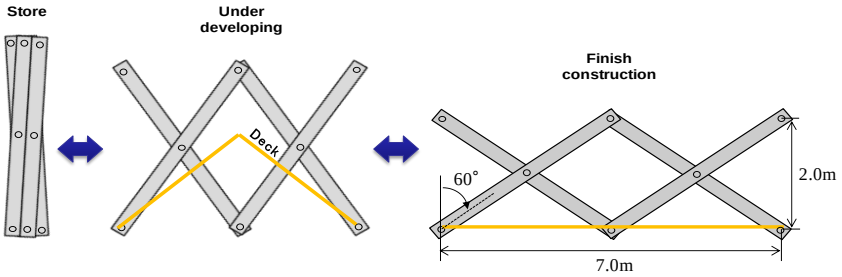

Figure 1: The stretching behavior of MB1.0.

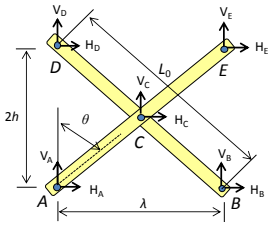

Figure 2: FBD of a unit scissors structure.

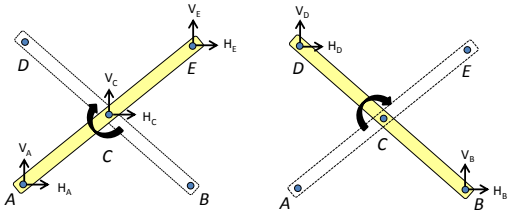

Figure 3: Continuity conditions of each member.

plastic bending moment is 20.1kNm, and the ultimate bending strength is 39.9kNm. The deck on which vehicles travel (called the aluminum alloy deck, hereafter) consists of A6063 extrusion sections. Only the portion of the aluminum alloy deck on which wheel loads act was constructed, because of weight saving. Moreover, the deployment action aims at shortening the construction time by uniting and interlocking the scissors member and the aluminum alloy deck. The properties of the A6N01 material are: E=61.0GPa, σ_B=198.8MPa, and σ_y=180.0MPa, while for the A6063 material E=68.0GPa, σ_B=150.0MPa, and σ_y=110.0MPa.

3 The Theory of scissors mechanism

3.1 Mechanics of a unit scissors structure

A Free Body Diagram (called FBD) for a unit of scissors structure is shown in Fig. 2. When the length of the members is L_0 and the angle of inclination is θ, the sectional length λ and height $2h$ are $L_0\sin\theta=\lambda$ and $L_0\cos\theta=2h$. So, the construction and storage of such a structure can be shown by the angle θ. This unit scissors structure can be designed by using the equation of equilibrium. The equation of equilibrium concerning each the external force V_A - V_E and H_A - H_E is given as two expressions,

$$\sum H = H_A + H_B + H_C + H_D + H_E = 0, \quad (1)$$

$$\sum V = V_A + V_B + V_C + V_D + V_E = 0 \quad (2)$$

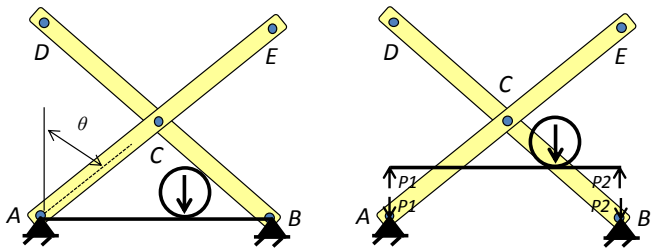

(a) Whole system (b) FBD of the deck

Figure 4: FBD of a unit scissors structure with deck.

Looking at the members *AE* and *BD* that intersect as shown in Fig. 3, it is obtained that the two equilibrium equations of moments occur at Point *C* as follows.

$$\text{Member of AE}: M_C = -hH_A + \frac{\lambda}{2}V_A = -hV_E + \frac{\lambda}{2}V_E, \tag{3}$$

$$\text{Member of BD}: M_C = hH_B + \frac{\lambda}{2}V_B = hV_D + \frac{\lambda}{2}V_D \tag{4}$$

Let's consider the case of cantilever model which is pinned support for point A and point D. It is possible to use the matrix by arranging the four calculated equilibrium equations eqn (1) - eqn (4) as shown in eqn (5).

$$\begin{bmatrix} 1 & 0 & 1 & 0 \\ 0 & 1 & 0 & 1 \\ -2h & \lambda & 0 & 0 \\ 0 & 0 & 2h & \lambda \end{bmatrix} \begin{Bmatrix} H_A \\ V_A \\ H_D \\ V_D \end{Bmatrix} = -\begin{bmatrix} 1 & 0 & 1 & 0 \\ 0 & 1 & 0 & 1 \\ 0 & 0 & 2h & -\lambda \\ -2h & -\lambda & 0 & 0 \end{bmatrix} \begin{Bmatrix} H_B \\ V_B \\ H_E \\ V_E \end{Bmatrix} - \begin{Bmatrix} H_C \\ V_C \\ 0 \\ 0 \end{Bmatrix} \tag{5}$$

Similarly, we can get equilibrium as eqn(6) in the simple beam model which is pinned support for point A and point B,

$$\begin{bmatrix} 1 & 0 & 1 & 0 \\ 0 & 1 & 0 & 1 \\ -2h & \lambda & 0 & 0 \\ 0 & 0 & 2h & \lambda \end{bmatrix} \begin{Bmatrix} H_A \\ V_A \\ H_B \\ V_B \end{Bmatrix} = -\begin{bmatrix} 1 & 0 & 1 & 0 \\ 0 & 1 & 0 & 1 \\ 0 & 0 & 2h & -\lambda \\ -2h & -\lambda & 0 & 0 \end{bmatrix} \begin{Bmatrix} H_D \\ V_D \\ H_E \\ V_E \end{Bmatrix} - \begin{Bmatrix} H_C \\ V_C \\ 0 \\ 0 \end{Bmatrix} \tag{6}$$

From the above results, unknown reaction forces can be obtained by considering the loading condition and the boundary condition for these.

3.2 Mechanics of a scissors structure in the consideration of deck

Next, let us consider the mechanical model when adding the deck to the fundamental theory of the scissors structure, as discussed in the previous section. The unit scissors model with the deck is shown in Fig. 4(a), and the FBD, which is made of the unit scissors and each independent deck, is shown in the Fig. 4(b).

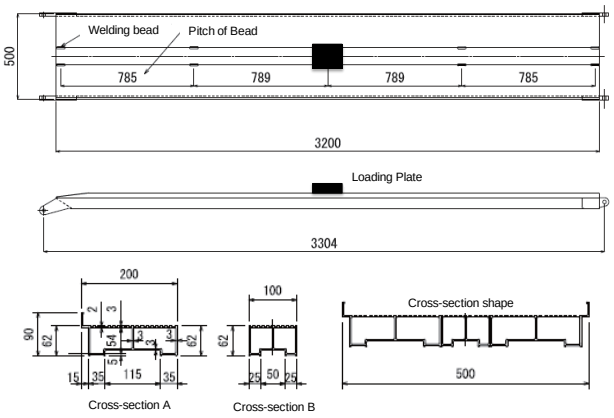

Figure5: The schematic diagram of deck.

Fig. 4(a) shows the whole of structure with moving load such as a vehicle. A vehicle passes over the deck between nodes *A* and *B*. According to the wheel load, the reaction forces on the supports occur in the deck, as shown in Fig. 4(b). The reaction force which arose in the deck is transmitted to the main member of a unit scissors as an external force *P*1 and *P*2. Because the wheel load transmitted from the deck changes with wheel positions, it is thought that the stress distribution which occurs for the scissors member and the deck changes depending on the positions of the vehicles.

4 Experimental evaluation of the load-carrying capacity of the aluminium alloy deck

This section describes the ultimate strength test for deck and its results in order to check the safety of the aluminum alloy deck under vehicle loading.

4.1 Outline of the aluminum alloy deck

The aluminum alloy deck with a vehicle traveling is shown in Fig. 5. The length of the deck is 3200mm and the width of the deck is 500mm. The type of material is A6063-T5. The deck is formed by welding two types of hollow extrusions, one with a width of 200mm and the other with a width of 100mm. The weight of one panel is 490N.

4.2 Experiment conditions

The aluminum alloy deck was constructed of a steel pipe of φ=20mm which was pin-fixed at both ends. The loading plate, which supports a tire contact area, uses 175mm*175mm steel plate and the rubber board according to guidelines of Eurocode for bridge design.

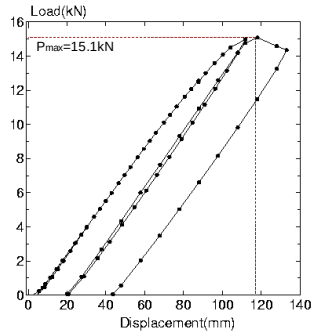

Figure 6: Load – displacement curve.

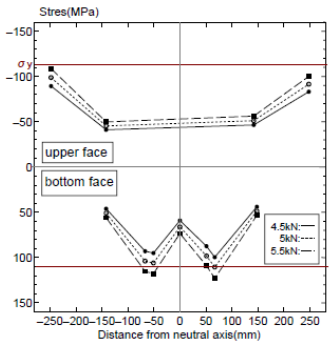

Figure 7: Distribution of the strain values at central section of the deck.

4.3 Experimental results

The load-displacement curve at the loading point is shown in Fig. 6. The horizontal axis shows the displacement of the head part of the loading machine, and the vertical axis shows the increment of the load. Below P=1kN, the load was increased by 0.2kN, and above P=1kN, the load was increased by 1kN until P=14kN. After reaching P=14kN, the load was removed and residual displacement and strain of the aluminum alloy deck was checked. Then, the displacement was increased by δ=10mm. The aluminum alloy deck had lost a load bearing capacity at the value of load of 15.1kN and the experiment ended.

4.4 Distribution of the stress in the central cross-section position

The stress distribution in the central section corresponding to the force of P=4.5kN, 5.0kN, and 5.5kN is depicted in Fig. 7 The stress values (MPa) are shown on the vertical axis, and the distances from the neutral axis (mm) are shown on the horizontal axis. Moreover, the line of σ_y=±110MPa shows the yield stress of the material A-6063. From Fig. 7, we can see that the undersurface surrendered for the first time at the value of force of P=5.0kN and the serviceability limits load of the deck was equal to 5.0kN. The maximum bending moment was M_{max} =28.7kNm in the central part of the aluminum deck, and this value corresponds to yielded bending moment for the deck.

5 The vehicle loading test using MB1.0

This section describes the outlines and results of the vehicles loading test using MB1.0. Moreover, experimental results are compared with theory of scissors and FE analysis.

5.1 Vehicles outline

Table 1: Loading conditions.

Load case	Type of vehicle	Loading condition(kN)		
		Total	Front axis	Rear axis
1	STREET	9.6	5.2	4.4
2	AD Van	13.8	7.5	6.3

Table 2: Vehicles stop positions.

Case	Vehicle stop position	
A	Front wheel	Center of first slab
B	Wheel axis	Center of first slab
C	Front wheel	Center of MB1.0
D	Wheel axis	Center of MB1.0
E	Rear wheel	Center of MB1.0

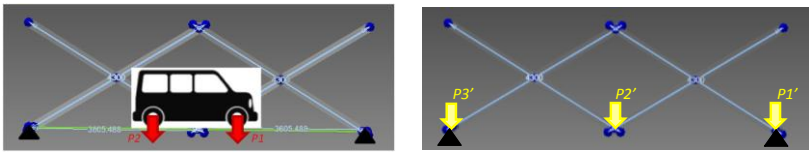

(a) Strict model (b) Simple model

Figure 8: 2D analytical model.

Two kinds of vehicles, Honda STREET and Nissan AD van, were used for the vehicles loading test. The STREET's (Full length*full width*overall height) was (3195mm*1395mm*1870mm), while the AD van's (Full length*full width*overall height) was (4370mm*1895mm*1510mm). The wheel base of the STREET was 1900mm and the total weight of the STREET including the driver is 9.6kN distributed 5.2kN of front axis and 4.4kN of rear axis. The wheel base of AD van was 2535mm and the total weight of the AD van including the driver is 13.8kN distributed 7.5kN of front axis and 6.3kN of rear axis.

5.2 Vehicles stop position and loading condition

From Tab 1 it can be seen that the measurements were performed five times. When the front wheel, the axle (defined here as the intermediate part of the front and the rear wheel), and the rear wheel came to a specific point and stopped, the value of the strain was measured. The stop positions were the center of the deck for the first unit scissors and the central part of MB1.0. Two cases of loads were considered, as seen in Tab 2. One case corresponds to the STREET, which is a light vehicle, and the other case is the AD van, which is a standard-sized car. In the loading Case 2, the additional weight was added from Case 1 was the backseat of the vehicles.

5.3 Verification of the frame analysis

We analyzed the MB1.0 model by Autodesk Inventor. The analysis was possible by using internal programming (ANSYS) embedded in CAD software. A beam element was used for all elements of the bridge. The analysis was conducted for to the Case *D* in Tab.2, in which maximum strain occurred for the vehicles in the stop position.

The models used in the numerical analysis are shown in Fig. 8. The dead load consists of the main member, the shaft, and the deck. Fig. 8 (a) is the strict model considering the deck, and Fig. 8 (b) is the simple model neglecting the deck. The

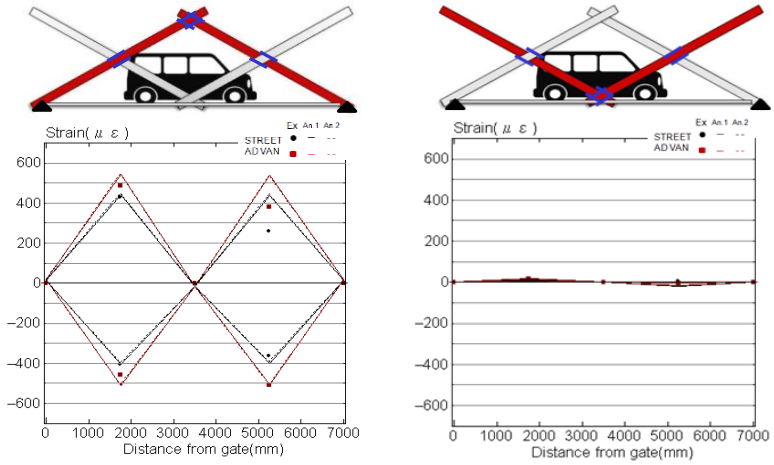

(a) Member ends-supports (b) Member ends-free

Figure 9: Distribution of strain in the center of MB1.0.

strict model made the wheel load on the deck in vehicle stopped positions, as shown in Fig. 8 (a). The simple model made the wheel load on the pin, as equivalent nodal forces, as seen in Fig. 8 (b). The live load depicted by the red arrow acts according to the wheel load, and the yellow arrow indicates the equivalent nodal force. As a boundary condition, the shaft part is pin-fixed at both ends.

5.4 Results of the experiment

Fig. 9 (a) and (b) shows the strain distribution in case when the vehicle was located in the center of the bridge. Fig. 9 (a) portrays a mountain-shaped member which starts from supports, and Fig. 9 (b) pays attention to the member which is in a free state (the target colored in red). Moreover, a blue mark in the figure shows the position of the strain gage. It can be seen that the experimental and analytical values are smaller than maxima admissible strain (=2000με) for loading vehicles until 13.8kN. A maximum strain of about 500με occurred in member intersection part, so the safety ratio was relatively large from the yield strain.

From Fig. 9 (a), we can confirm that the maximum strain of 500με was measured at the circumference of the pivot of the first unit, and the minimum strain was measured by the circumference of the pivot of the second unit. Because the distribution of the strain was almost equal in the compression and the tension area, it turned out that the influence of the bending moment was great. Although accuracy had variations in comparison with the analytical results, the maximum value was distributed within 10%.

Fig. 9 (b) shows that strains hardly occurred at the member, which was in an end-free state (maximal value around ±10με). It turned out that the analytical results also showed the same tendency. The bending moment did not act on the

member, but the strain had increased with a little axial tension.

Conclusion

The points which became clear from this research are followed as:

1) Through the bending test, it was proved that the load-carrying capacity of the aluminum deck was sufficient for vehicles passing over.
2) In the static loading experiment of MB1.0 it was found that measured strains caused by vehicles loading are consistent with previously obtained analytical values (difference less than 10%).
3) With a maximum loading weight of 13.8kN, the main member and decks are within allowable stress, and it turned out that the vehicles about 10kN could pass safely on MB1.0.

Acknowledgments

This research was supported for Dr. I. Ario by a Grant-in-Aid-Scientific-Research Base Research (B) of JSPS in 2011 - 2013. We appreciated that all manufacture of cradles were supported by Akashin Corporation in Japan. We appreciated that all experiments were supported by Japan Construction Method and Machinery Research Institute. Moreover, we appreciate that a sample of the aluminum materials were offered by Star Light Metal Industry Co., Ltd. in Japan.

References

[1] J. Holnicki-Szulc, P. Pawlowski, and M. Wiklo: High-performance impact absorbing materials - the concept design tools and applications, Smart Materials and Structures: Int. J. Non-Linear Mechanics, pp. 461-467, 2003.
[2] I. Ario and A. Watson: Structural Stability of Multi-Folding Structures with Contact Problem: *Int. J. Non-Linear Mechanics*, Vol.324 (1-2), pp.263-282.
[3] I. Ario and M. Nakazawa: Nonlinear Dynamics behavior of Multi-Folding Microstructure Systems based on Origami Skill: *Int. J. Non-Linear Mechanics*, Vol. 45(4), pp. 337-347, 2010.
[4] I. Ario and H. A. Kim: Michell Problem for the Stiffness Formation of Structural Design in 3 Dimensional Space: *Proc. of Optimizational Symposium in JSME*, 7, pp.179-184, 2006.
[5] I. Ario: Structure with the expanding and folding equipment as a patent (No.2006-037668), 2006.
[6] I. Ario, Y. Tanaka, M. Nakazawa, Y. Furukawa and Y. Chikahiro: Research and development of the high-efficiently foldable structure (Analysis), *Proc. of Space Structure and Material Symposium in JAXA*, Vol. 25, pp. 104-107, 2009, (in Japanese).
[7] Y. Tanaka, I. Ario, M. Nakazawa, Y. Furukawa and Y, Chikahiro: Research and development of the high-efficiently foldable structure (Experiment),

Proc. of Space Structure and Material Symposium in JAXA, Vol. 25 pp. 108-111, 2009 (in Japanese).

[8] I. Ario, Y. Tanaka, M. Nakazawa, Y. Furukawa and Y. Chikahiro: Development of the prototype of a new emergency bridge based on the concept of optimized structure, *Journal of Structural Engineering, JSCE*, Vol. 64A, pp. 1-12, 2010 (in Japanese).

[9] I. Ario, Y. Furukawa, Y. Tanaka, Y. Chikahiro, S. Matumoto, M. Nakazawa, I. Tanikura and S. Ono: Dynamic Vibration of a Prototype Deployable Bridge based on MFM, *The proceedings of the 9th World Congress on Computational Mechanics and 4th Asian Pacific Congress on Computational Mechanics WCCM*/APCOM, CD, 2010.

[10] M. Nakazawa and I. Ario: Mechanical Property of Deployable Emergency Bridge Based on the Scissors Structures, *Journal of safety problems*, Vol. 5 pp. 133-138 , 2010 (in Japanese).